JOURNAL OF GEOPHYSICAL RESEARCH, VOL. 108, NO. A6, 1233, doi:10.1029/2002JA009339, 2003

# Shock front nonstationarity of supercritical perpendicular shocks

Tohru Hada and Makiko Oonishi

Department of Earth System Science and Technology, Kyushu University, Fukuoka, Japan

Bertrand Lembège and Philippe Savoini

Centre d'étude des Environnements Terrestre et Planétaires, CNRS, Université de Versailles Saint-Quentin-en-Yvelines, Vélizy, France

Received 21 February 2002; revised 30 September 2002; accepted 29 January 2003; published 12 June 2003.

[1] The shock front nonstationarity of perpendicular shocks in super-critical regime is analyzed by examining the coupling between "incoming" and "reflected" ion populations. For a given set of parameters including the upstream Mach number ($M_A$) and the fraction $\alpha$ of reflected to incoming ions, a self-consistent, time-stationary solution of the coupling between ion streams and the electromagnetic field is sought for. If such a solution is found, the shock is stationary; otherwise, the shock is nonstationary, leading to a self-reforming shock front often observed in full particle simulations of quasi-perpendicular shocks. A parametric study of this numerical model allows us to define a critical $\alpha_{crit}$ between stationary and nonstationary regimes. The shock can be nonstationary even for relatively low $M_A$(2–5). For a moderate $M_A$(5–10), the critical value $\alpha_{crit}$ is about 15 to 20%. For very high $M_A$ (>10), $\alpha_{crit}$ saturates around 20%. Moreover, present full simulations show that self-reformation of the shock front occurs for relatively low $\beta_i$ and disappears for high $\beta_i$, where $\beta_i$ is the ratio of upstream ion plasma to magnetic field pressures. Results issued from the present theoretical model are found to be in good agreement with full particle simulations for low $\beta_i$ case; this agreement holds as long as the motion of reflected ions is coherent enough (narrow ion ring) to be described by a single population in the model. The present model reveals to be "at variance" with full particle simulations results for the high $\beta_i$ case. Present results are also compared with previous hybrid simulations. *INDEX TERMS:* 7843 Space Plasma Physics: Numerical simulation studies; 7851 Space Plasma Physics: Shock waves; 6939 Radio Science: Magnetospheric physics; 7514 Solar Physics, Astrophysics, and Astronomy: Energetic particles (2114); *KEYWORDS:* collisionless shocks, nonstationarity effects, nonlinear physics, particles acceleration, particles thermalization, terrestrial and planetary shocks

**Citation:** Hada, T., M. Oonishi, B. Lembège, and P. Savoini, Shock front nonstationarity of supercritical perpendicular shocks, *J. Geophys. Res.*, *108*(A6), 1233, doi:10.1029/2002JA009339, 2003.

## 1. Introduction

[2] It is well documented that the main dissipation source required to complete a collisionless quasi-perpendicular shock in a magnetized plasma varies mainly according to the upstream Mach number, $M_A$. In a subcritical regime, i.e. $M_A < M_A^*$, where $M_A^*$ is the so-called critical Mach number (= 2–3 when typical solar wind plasma conditions are used), resistivity alone can provide enough dissipation to support the stationary shock structure. The anomalous resistivity is thought to be provided by various current instabilities driven by the electric current generated at the thin shock ramp, whose width is of the order of the resistive scale length.

[3] On the other hand, in a super-critical regime ($M_A > M_A^*$), an additional source of dissipation is required in order to satisfy the Rankine-Hugoniot jump relations across the shock, and to get a stationary downstream state. From a fluid point of view, it can be shown that this additional dissipation should be provided by viscosity. However, due to the nonlocal nature of the viscous interaction in a collisionless plasma, it turns out that the viscous dissipation does not take place in the same manner as the resistive dissipation: instead of having a steep ramp over the ion viscous scale length, a substantial fraction of upstream ions are reflected at the shock front. During their reflection, ions are accelerated by the motional electric field, gyrate back to the shock front, and are then transmitted downstream without any further reflection. These once-reflected ions and directly transmitted ions are rapidly mixed by downstream plasma turbulence, and the downstream ion temperature is effectively enhanced. This provides an extremely efficient way of the viscous heating.

[4] As it is expected from the above description, the nature of this kinetic viscous dissipation for super-critical collisionless shocks strongly depends on properties of the


0148-0227/03/2002JA009339$09.00

reflected ions. Unlike fluid, local description of the kinetic dissipation via the reflected ions can be much more dynamic, and there is no guarantee that a stationary shock structure can be obtained under given parameters. In fact, it has been known for almost three decades that, in many full particle simulations, in which both ions and electrons are treated as macro-particles, quasi-perpendicular shocks are characterized with nonstationarity of the shock front, i.e. by self-reformation of the front. The reflected ions accumulate in front of the ramp, and form the foot in the magnetic field and the ion density profile. Concentration of the magnetic field and the density self-consistently produce the electric field in such a way that new incoming ions are decelerated. As time goes on, more and more reflected ions accumulate, and the amplitude of the normal electric field (or the potential) grows large enough to start reflecting substantial number of the incoming ions, leading to the formation of a new shock front, at a location about a foot length in front of the original shock front. This entire process is repeated periodically [*Biskamp and Welter*, 1972; *Lembège and Dawson*, 1987; *Lembège and Savoini*, 1992].

[5] In this paper, we analyze the conditions for which the nonstationarity or stationarity of the shock front occurs, using a model similar to the well-known hybrid numerical simulation model, and to compare the results with those obtained by full particle numerical simulations. The paper is organized as follows. Section 2 will summarize numerical conditions used for full particle simulation and corresponding main results (used as references). Section 3 describes the new hybrid-type numerical model. Section 4 will include the main results and discussion, while conclusions will be presented in section 5.

## 2. Conditions of Numerical Simulations

[6] Initial and boundary conditions used in the present 1-*D* electromagnetic full particle simulations are identical to those already explained in detail by *Lembège and Savoini* [1992]; the shock is initiated by a magnetic piston (applied current pulse). Briefly, the shock is propagating along *x* axis, and a static magnetic field $B_o$ is applied along z axis (perpendicular shock). All dimensionless quantities are indicated by a tilde "~" and are normalized as follows. The spatial coordinate is $\tilde{x} = x/\Delta$; velocity $\tilde{V} = V/\omega_{pe}\Delta$; momentum of species $\gamma$, $\tilde{p}_\gamma = p_\gamma/m_e\omega_{pe}\Delta$; electric field $\tilde{E} = qE/m_e\omega_{pe}^2\Delta$; magnetic field $\tilde{B} = qB/m_e\omega_{pe}^2\Delta$; time $\tilde{t} = \omega_{pe}t$. The parameters $\Delta$, $\omega_{pe}$, $m_e$, $q$ and $n_o$ are, respectively, the numerical grid spacing, the electron plasma frequency, the electron mass, the electric charge and the particle density at t = 0.

**Table 1.** Upstream Plasma Parameters Defined for Full Particle Simulations (Figures 1 and 2)

| | Electrons | Ions |
|---|---|---|
| $\tilde{v}_{th}$ | 0.2 | 0.017 |
| $\tilde{\lambda}_D$ | 0.2 | 0.16 |
| $\tilde{\rho}_c$ | 0.4 | 2.91 |
| $\tilde{c}/\tilde{\omega}_p$ | 3 | 27.5 |
| $\tilde{\omega}_c$ | 0.5 | 0.006 |
| $\tilde{\omega}_p$ | 1 | 0.11 |
| $\tilde{\tau}_c$ | 12.55 | 1055.46 |
| $\beta$ | 0.0355 | 0.0225 |

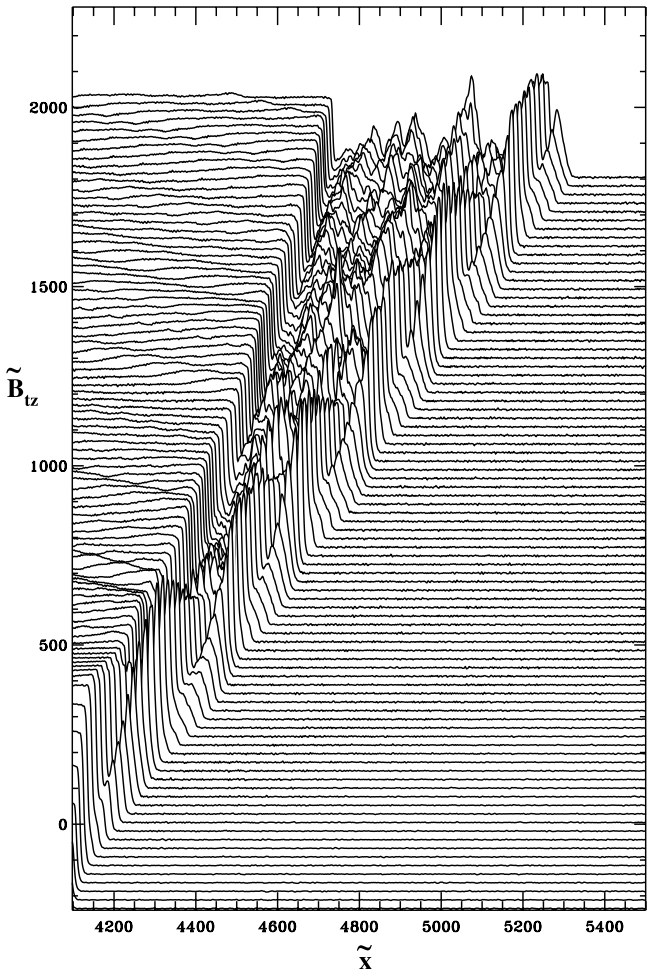


**Figure 1.** Stackplots of the main magnetic field $\tilde{B}_{tz}$ at different times of the run from $\tilde{t}$ = 24 to 2064. The shock is propagating from the left-hand to the right-hand side. Time interval between two successive curves is $\tilde{t}$ = 24; ion $\beta_i$ = 0.022. Cycles of the shock reformation are well evidenced.

[7] The basic parameters are plasma box size length $L_x$ = 4096; velocity of light $\tilde{c}$ = 3, mass ratio $m_e/m_i$ = 0.0119. At t = 0, the particle density is $n_e = n_i = 50$ at each grid point and the temperature ratio is $T_e/T_i$ = 1.58, the magnetic field $|B_o|$ = 1.5.

[8] For these initial conditions, the plasma parameters are summarized in Table 1 for both electrons and ions. The shock is propagating in a supercritical regime ($M_A$ = 3.07), where $M_A = \tilde{V}_{shock} / \tilde{V}_A$ has been determined in the upstream plasma (i.e. simulation) frame; the Alfven velocity $\tilde{V}_A$ is equal to 0.16. The size of the box allows to follow the shock and particles dynamics over a time $\tilde{t} \approx 2\tilde{\tau}_{ci}$ (or equivalently $12.56\omega_{ci}^{-1}$), where $\tilde{\tau}_{ci}$ is the upstream ion gyroperiod.

[9] Figure 1 illustrates the reformation cycle in the magnetic component $\tilde{B}_{tz}$, while Figure 2 shows the ion phase space and the normal electrostatic field $\tilde{E}_{lx}$ versus $\tilde{x}$ at different times of the fifth reformation cycle identified in Figure 1 (i.e., $\tilde{t}$ = 1568–1920).

[10] At time $\tilde{t}$ = 1584, the shock front is at about $\tilde{x}$ = 5000, and the reflected ions start accumulating in front of the ramp (Figure 2a). Later on ($\tilde{t}$ = 1632 and 1704), their density increases and a local $E_{lx}$ field is growing up in the

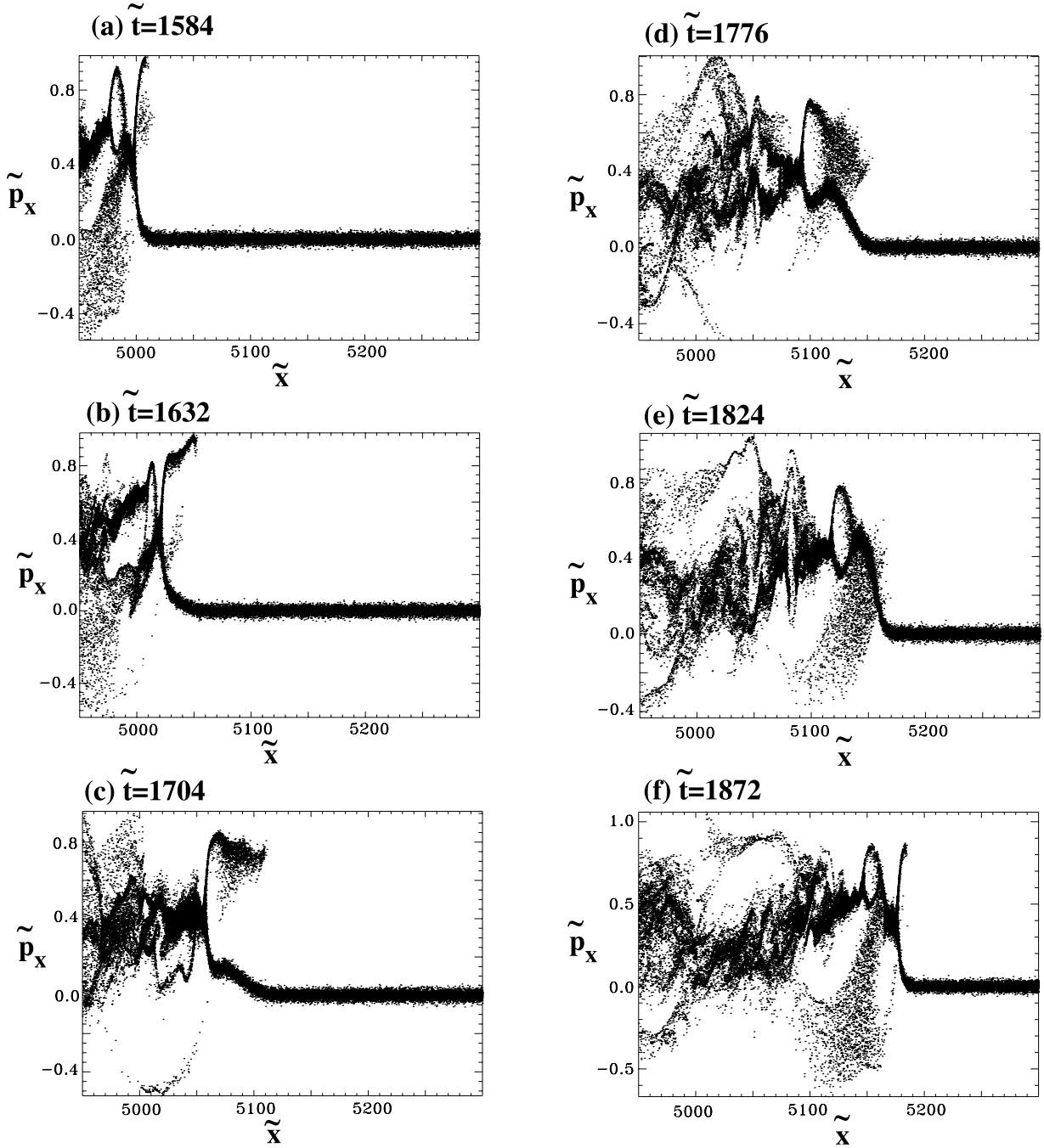


**Figure 2a.** Ion phase space $\tilde{p}_x$ versus $\tilde{x}$ at different times of the run within one cyclic self-reformation of the shock front from $\tilde{t}$ = 1568 to 1920 for ion $\beta_i$ = 0.022.

foot (Figure 2b), in such a way that new incoming ions are accelerated (in the present reference frame where the upstream plasma is at rest); simultaneously, the $E_{lx}$ field amplitude decreases at the overshoot. At $\tilde{t}$ = 1824, the new shock front is well formed around $\tilde{x}$ = 5150; ions reflected from this newly generated shock front already start to accelerate new incoming ions ($\tilde{t}$ = 1872).

[11] One arguable point about this self-reformation of supercritical shocks front is that the same phenomena has not been reported by hybrid simulation studies to date, in which the ions are treated as particles but the electrons are described as a massless fluid. To be strict, some nonstationary behavior of quasi-perpendicular shocks (but without reformation) has been in fact observed in hybrid simulations, when different values of upstream $\beta$ (= ratio of plasma to magnetic field pressures) have been used [*Leroy et al.*, 1981, 1982]. However, these particular shocks with upstream $\beta \approx 1$ do not represent the self-reformation of the shock front being discussed here (where $\beta \ll 1$). Some tentatives for reconciling full particle and hybrid results have been performed recently [*Lembège and Simonet*, 2001]. One key result is that a readjustment of scales and plasma parameters (mesh grid size $\Delta$, ratio $\omega_{pe}/\omega_{ce}$, values of $T_e$ and $\beta_e$) is necessary to realize such a reconciliation.

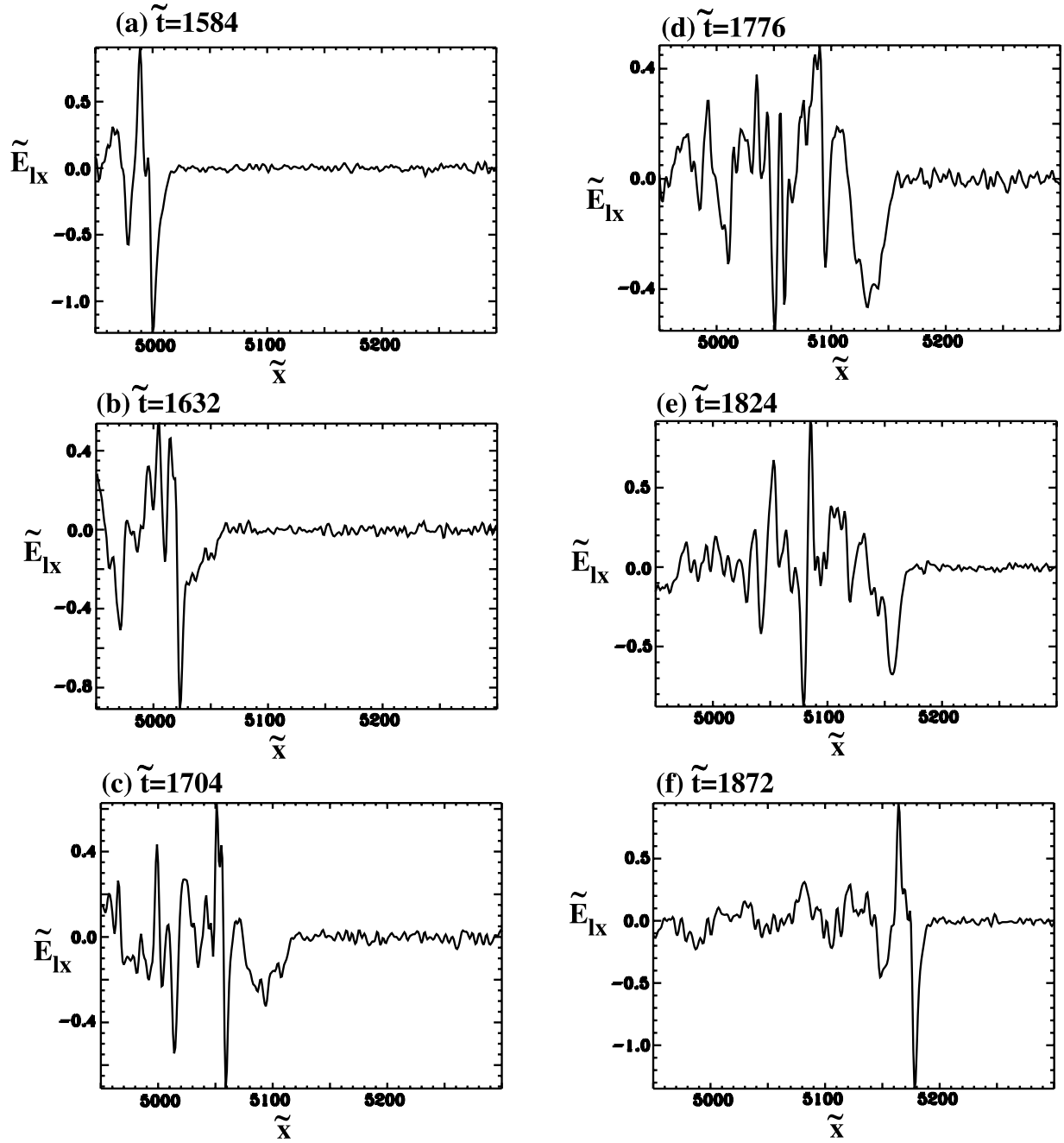


**Figure 2b.** Corresponding x-profiles of the electrostatic field $E_{lx}$.

These parameters may affect the appropriate resolution for defining the thickness of the ramp, and consequently, the local conditions for ion reflection. In particular, the ramp width $\Delta_r$ can self-consistently adapt according to the local dissipation need in full particle simulations so that $\tilde{c}/\tilde{\omega}_{pe} < \Delta_r < \tilde{c}/\tilde{\omega}_{pi}$, while its smallest physical scale is commonly limited to the ion inertia length $\tilde{c}/\tilde{\omega}_{pi}$ in hybrid simulations. One noticeable feature is that fields components fluctuate at the overshoot (i.e. at a given place x) in hybrid results (Figure 11 of *Leroy et al.* [1982]), while these fluctuations take place alternatively both at the overshoot and foot, i.e. over a finite space scale including both ramp and the foot widths, as shown in present Figure 1. However, in both cases, fields fluctuations period is of the order of the ion gyroperiod. This suggests that a similar process is under way but is more or less evidenced (i.e. is spreading over different spatial scales) according to the scales readjustment mentioned by *Lembè*ge and Simonet [2001]. This point will be analyzed later on. One has also to notice that there is a noticeable difference in the fraction of reflected ions, $\alpha$, between the full particle and the hybrid simulation results. For typical quasi-perpendicular shocks with moderate Mach numbers, $\alpha$ is 18 to 25 percent in full particle simulations, while it is about 13 percent or less for $M_A$ below 6 in hybrid simulations (Figure 12 of *Leroy et al.* [1982]).

[12] Since the real value of $\alpha$ must be self-consistently determined using full three-dimensional dynamics of both ions and electrons at the shock ramp (with a realistic mass

ratio), we are not, at present time, in a position to analyze in detail the differences of $\alpha$ determined by the two types of simulations. Instead, herein, we take the value of $\alpha$ as a free parameter, and discuss whether the stationarity of the perpendicular shock in fact can be ascribed to the different values of $\alpha$.

## 3. Formulation of the Numerical Model

[13] In this section, we model the macro-structure of perpendicular shocks in the supercritical regime by using a method similar to the hybrid model. Unlike the usual hybrid simulation studies, we do not solve time evolution of the system: instead, we seek for by iteration a self-consistent, time-stationary configuration of the incoming and reflected ion streams, charge-neutralizing electron fluid, and the electromagnetic field, by solving simultaneously the equations of motion of ions and the electron fluid, and the Maxwell's equations.

[14] Let us consider a perpendicular, supercritical shock, with its ramp situated at $x = 0$, with $x$ positive and negative corresponding to upstream and downstream, respectively. We assume that all the physical variables depend only on the main coordinate, $x$, and that the magnetic field orientation is along the $z$-axis. We normalize all the physical variables using the static magnetic field ($B_0$), the ion cyclotron angular-frequency, the Alfven speed ($V_{A0}$), and the plasma density, all defined at a certain reference point far upstream of the shock, except for the electric field, which is normalized to $V_{A0}B_0/c$, where $c$ is the light speed.

[15] Now we can write down governing equations in the normalized unit. Ion trajectories are derived by time integration of motion equations,

$$\frac{dX_j}{dt} = V_{xj}; \tag{1a}$$

$$\frac{dV_{xj}}{dt} = E_x + V_{yj}B; \tag{1b}$$

$$\frac{dV_{yj}}{dt} = E_y - V_{xj}B \tag{1c}$$

where $j$ denotes the particle number, $X$ and $V$ are the position and the velocity of individual ions, $\mathbf{E} = (E_x, E_y, 0)$ is the electric field, and $\mathbf{B} = (0, 0, B)$ is the magnetic field, respectively. Note that even though we are dealing with the time-stationary solution, the above equations are still meaningful: the variable '$t$' may be interpreted as an implicit parameter to determine the ion trajectories. The equation of motion of a fluid, massless electron, together with the Ampere's law, leads to,

$$0 = -n\left(E_x + U_yB + \frac{B}{n}\frac{dB}{dx}\right) - \frac{dP_e}{dx}; \tag{2a}$$

$$E_y - U_xB = 0, \tag{2b}$$

where $n(x)$ is the density (quasi-neutrality assumed), $\mathbf{U} = (U_x, U_y, 0)$ is the ion bulk velocity, and $P_e$ is the electron pressure, respectively. From Lorenz's law, we have $E_y$ = constant. Also, from equation (2b) and from the continuity equation of ions, we have $n = B$ everywhere (in our normalization), which is a natural consequence of a system where the magnetic field is orthogonal to the spatial coordinates of the system and purely compressional. If we assume for simplicity the electron fluid to be isothermal, i.e., $P_e = nT_e$, with $T_e$ being the electron temperature, equation (2a) can be rewritten as

$$E_x = -U_yB - \frac{dB}{dx} - 2\beta_e\frac{d\log n}{dx} \tag{3}$$

where $\beta_e$ is the electron beta ratio.

[16] Using the equations above, actual computations were carried out in the following manner:

[17] 1. Specify a set of parameters including upstream Mach number ($M_A$), the fraction $\alpha$ of reflected to incoming ions densities, the thermal spread of the incoming ($V_{ti}$) and of reflected ($V_{tr}$) ion streams, and the electron beta ($\beta_e$). In this paper we only consider the case $V_{ti} = V_{tr} \equiv V_t$.

[18] 2. Using (1), compute trajectories of incoming and reflected ion streams which are introduced into the simulation system at a point far upstream (typically at around $x = 10$) with thermal spreads $V_{ti}$ and $V_{tr}$. We employ a square-shape distribution function for both ion streams as they are introduced into the system, i.e., the distribution function of the incoming ion stream is, $f_i(V) = 1/(2n_iV_{ti})$ for $-M_A - V_{ti} < V < -M_A + V_{ti}$, and $f_i(V) = 0$ otherwise, and likewise for the reflected ion stream. At the first cycle of the iteration, a "trial" electromagnetic field is used: $B(x) = 1$, $E_x(x) = 0$, and $E_y = M_A$ (the last relationship is exact).

[19] 3. Compute $n$, $U_x$, and $U_y$ as new macro-particles ions are introduced. We use a triangular shape function when we distribute the influence of the macro-particles to nearby grid points.

[20] 4. Renew the electromagnetic field by $B = n$ and (3). One can also compute $E_y$ using (2b), and monitor its constancy in order to check the validity of the computation.

[21] 5. Go back to step 2 and recompute the ion trajectories influenced by the new updated field. If the plasma and the field profiles converge after some iterations (we typically computed 200 cycles), we regard the shock to be time-stationary. Otherwise, the shock is classified as nonstationary. The number of iterations vary significantly depending not only on parameters but also on the first trial electromagnetic field. Thus, every time we make a run with a new set of parameters, we let it only slightly different from the set of parameters known to converge to a stable shock, and use its profile as the initial trial field.

## 4. Main Results and Discussion

[22] Figure 3a shows a case in which the time-stationary shock configuration is obtained after several iterations. Used parameters are $M_A = 4$, $\alpha = 0.1$, and $V_t = V_{ti} = V_{tr} = 0.2$, and $\beta_e = 0$. Left panels show the incoming and the reflected ions in the phase space $v_x - x$, and right panels show $B(x)$ (=$n(x)$) and the electric potential $\phi(x)$. Panels from the top (initial profiles) to bottom correspond to increasing number of iterations. The presence of the reflected ions increases the plasma density $n$, particularly at their turning point around

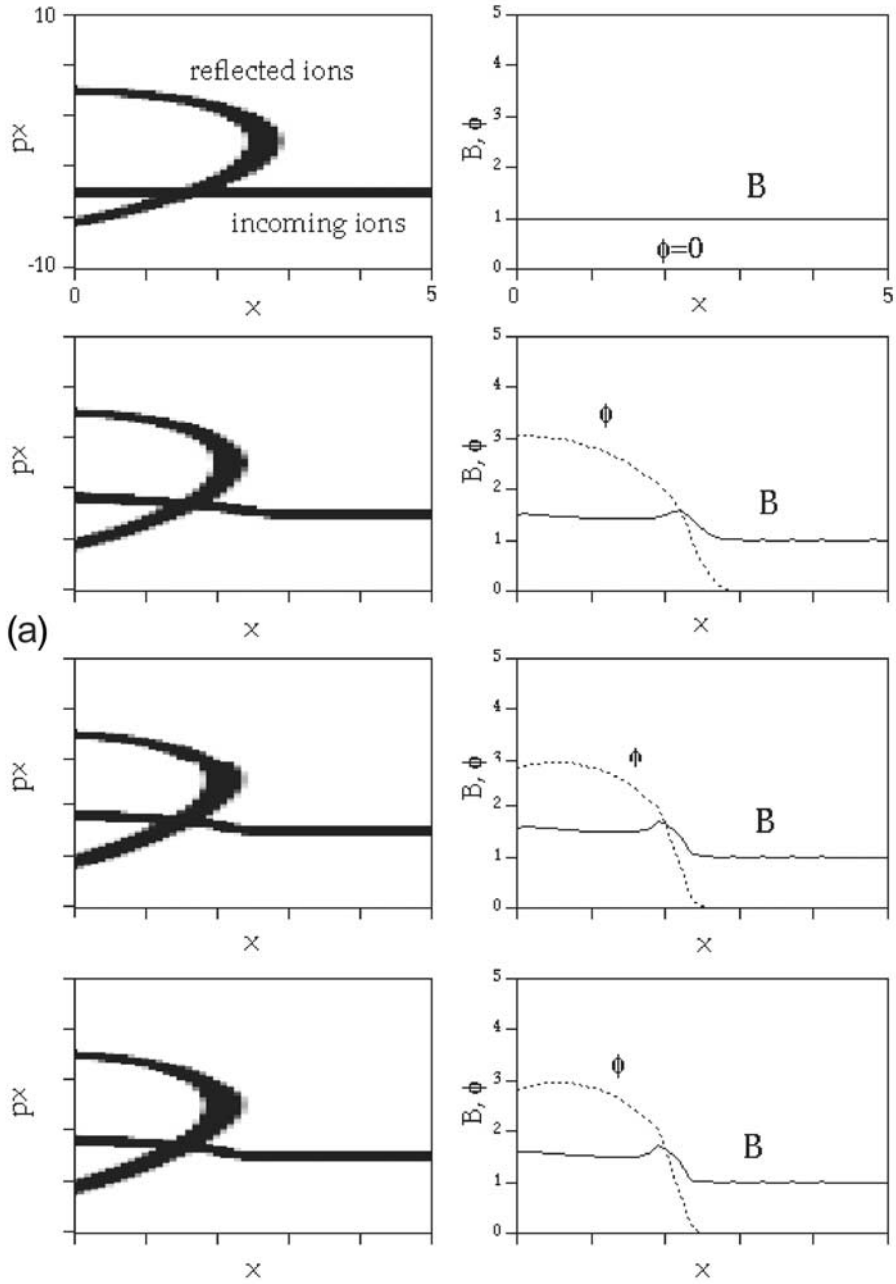


**Figure 3.** Ion phase space (left panels) and fields variables (right panels) shown as the number of iterations increases (from top to bottom panels). Results are issued from our present numerical model and are obtained for $M_A = 4$, when the fraction of reflected ions $\alpha = 0.1$ (case a) and 0.2 (case b); B and $\phi$ are respectively the magnetic field and the electrostatic potential. Upstream ion parameter $\beta_i = 0.67$, while $\beta_i = 0.07$ and 0.13 for reflected ions respectively in case a and b.

$x = 2.3$ (smeared by the thermal spread). This corresponds to a local hump of $B$. This magnetic compression, as well as the magnetic deflection of the incoming ion stream into $y$ direction (via the $E \times B$ drift) are well recovered [*Leroy*, 1983].

[23] In the second case (Figure 3b), the used parameters are the same as before except that $\alpha$ is increased to 0.2. Then, the deceleration of incoming ions (in the present reference frame where upstream plasma is in motion) is strong enough to separate the incoming and the reflected ions. In this case, the field profiles and the shape of ion streams are completely different from those in Figure 3a. Indeed, the two ion streams violently oscillate, sometimes cross over each other, as iteration continues. Since we are searching for a time-stationary solution, details of the evolution of the variables as iteration continues have no significant meaning. Rather, it is appropriate to say simply that under this particular choice of parameters, there is no time-stationary shock solution. Nevertheless, it is likely that this state corresponds to the shock with self-reforming front illustrated in Figures 1 and 2,

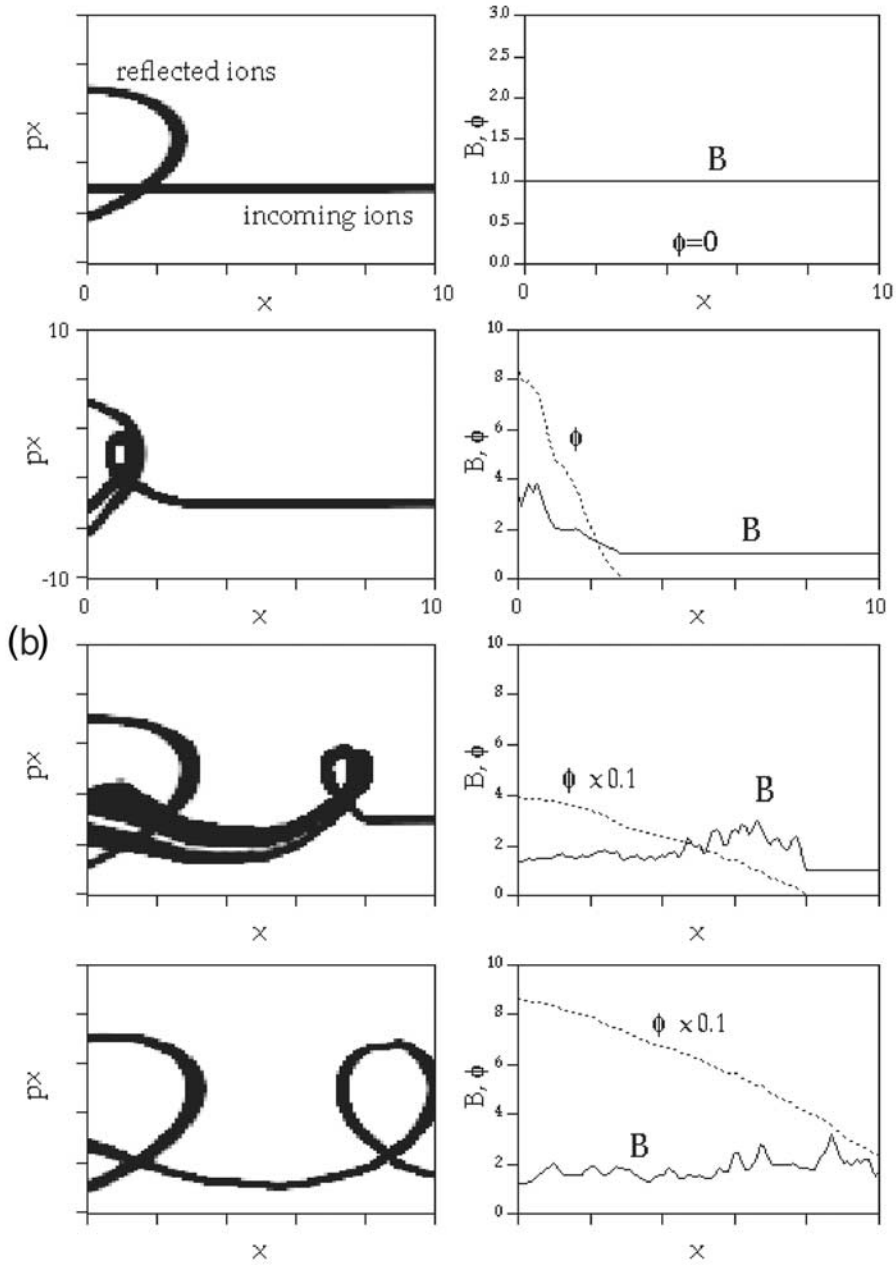


**Figure 3.** (continued)

since it is the strong coupling between the incoming and reflected ions that induces the reformation.

[24] By compiling many runs with different set of parameters, Figure 4 classifies in the phase space of $M_A$ and $\alpha$ the stationary and nonstationary shock regimes. Parameters used here are $V_t = 0.2$ and $\beta_e = 0$. A cross (circle) represents a run in which the computation ended (did not end) with a stationary shock profile. The solid curve shown in the figure denotes the critical percentage value $\alpha_{crit}$, which separates the two regimes. At $\alpha = \alpha_{crit}$, the shock is marginally stable.

[25] Dependence of $\alpha_{crit}$ on ion and electron upstream temperatures is summarized in Figures 5a and 5b. In Figure 5a, the ion thermal spread $V_t$ is varied. Since we are using the square-type distribution function for the ions, the beta ratio for the incoming and the reflected ions are approximately given as $2V_t^2/3B^2$ and $2\alpha V_t^2/3B^2$, respectively. In Figure 5b, the dependence of $\alpha_{crit}$ on $\beta_e$ is presented.

[26] Figures 4 and 5 provide several important pieces of information:

[27] 1. It evidences the existence of the critical $\alpha_{crit}$ for a wide $M_A$ range (still above $M_A^*$). For weak shocks (say, $M_A <$ 2–5), the stability depends on $M_A$, $\alpha$, and $V_t$. In contrast, the value of $\alpha_{crit}$ saturates for high $M_A > 10$, which means that stability of stronger shocks is mainly determined by $\alpha$ only. For typical planetary bow shocks, critical value $\alpha_{\rm crit}$ for marginal stationarity is about 20%.

[28] 2. A comparison of the present model with full particle simulation results of Figures 1 and 2 shows a very good

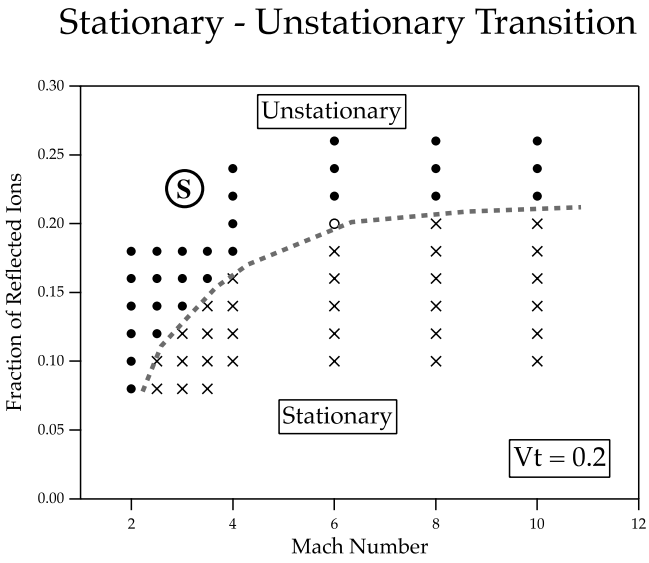


**Figure 4.** Summary of the parametric study performed with the numerical model for determining whether the shock front reformation takes place (nonstationarity) or not (stationarity), versus Mach number $M_A$ and the percentage $\alpha$ of reflected ions. The letter "S" indicates the result obtained from the present full particle simulation.

agreement (in the present case where the upstream ion $\beta_i$ is low). Indeed, self-reformation is well evidenced for $M_A$ = 3.07 (Figures 1 and 2), for which one measures a percentage $\alpha$ = 0.25 above the theoretical $\alpha_{crit}$ = 0.12 in Figure 4. In addition, several full particle simulations performed for different values of $M_A$ (not shown here) confirm such an agreement; previous simulation results of *Lembège and Dawson* [1987] and *Lembège and Savoini* [1992] also confirm this agreement.

[29] 3. The self-reformation is shown to depend mainly on the interaction between incident and reflected ions. Then, it does not depend (at least directly) on electrons dynamics, and in particular on the mass ratio. This supports previous results where self-reformation has been evidenced even for unrealistic mass ratios commonly used in full particle simulations. Then, similar results may be expected for further full particle simulations based on realistic mass ratio. The cyclic period of this self-reformation has been always found of the order of the mean ion gyroperiod measured within the ramp, in various simulations based on different mass ratios.

[30] 4. By increasing $\beta_e$, the critical percentage $\alpha_{crit}$ decreases. This is understandable since the electric field (or the force acting on the electrons) due to the compression of the magnetic field and that due to the electron fluid (the second and the third terms of the right-hand side of (3), respectively) have the same sign because $B = n$. Thus, $E_x$ is enhanced as the electron temperature effect is taken into account, and this results in the stronger coupling between the ion streams and the field, reducing $\alpha_{crit}$. However, the effect of $\beta_e$ in reducing $\alpha_{crit}$ is rather small for a wide range of $M_A$.

[31] 5. However, the present model is "at variance" with full particle simulations results for high ion $\beta_i$. Let us focus first on the model itself. This model stresses that the $\alpha_{crit}$ decreases as the ion temperature is increased, i.e. self-reformation should be more easily evidenced. This modification is somewhat larger compared with the electron temperature effect (note that, in Figure 5a, $V_{ti}$ = 0.2 and 1 approximately correspond to the ion beta of 0.03 and 0.67, respectively). Unlike the electron temperature effect, the interpretation of the dependence of $\alpha_{crit}$ on $V_{ti}$ is not straightforward. When an ion stream has a thermal spread, the ions will also spread in space, as they are deflected by the electromagnetic field. The effect is most eminent for the reflected ions around the turning point. The larger this spatial spread is, the less the density of the reflected ions and $E_x$ become; in contrast, the total potential difference $\Delta\phi$ between the shock site and far upstream, which basically is a product of $E_x$ and the spatial scale where $E_x$ is enhanced, remains not much influenced by $V_{ti}$. From our theoretical calculations we found that, the nonstationary shock occurs if (some portion of) the incoming ions are decelerated by $E_x$ so strongly that these ions are reflected back to the upstream region before reaching the shock. Namely, $u^2/2 > \Delta\phi$ for all the ions (where $u$ is the ion velocity) is the condition for the stationarity. Even when a small fraction of the incoming ions are reflected, they will trigger a large field perturbation, and eventually this leads to the nonstationarity. Since $M_A - V_{ti} < u < M_A + V_{ti}$, the larger the $V_{ti}$ is, it is more likely that the above inequality is satisfied, when we keep all the other variables fixed. Let us remind that reflected ions are described in the model by a single population with a given thermal velocity.

[32] The dependence of the model versus upstream ion $\beta_i$ is now compared with results issued from full particle simulations. Results are summarized in Figure 1 and Figure 6 which show stack plots of the main magnetic field component for different values of the ion temperature $T_i$. All other parameters are unchanged; in particular, same $M_A$ = 3.07 is used. It clearly appears that as the upstream ion $\beta_i$ increases (0.022, 0.177 and 0.35 respectively for Figures 1, 6a, and 6b), the self-reformation of Figure 1 disappears and tends to be replaced by time fluctuations of the fields at the overshoot (Figure 6a); this behavior is very similar to the case analyzed by *Leroy et al.* [1982] with hybrid simulation (Figure 11 of *Leroy et al.* [1982] where $\beta_i$ = 0.1 can be compared with present $\beta_i$ = 0.17). For higher $\beta_i$ (=0.35), the shock front becomes stationary (Figure 6b); this case should be compared with Figure 7 of *Leroy et al.* [1982] with higher $\beta_i$ (=1) where time fluctuations at the overshoot almost disappear. In other words, the thermal velocity of incident ions has a very strong impact on the shock front dynamics.

[33] This variation versus $\beta_i$ is in disagreement with that expected from our theoretical model. An explanation for this discrepancy may be found by analyzing the ion phase space for each case. Results are summarized in Figure 7, which shows the $p_{xi} - x$ phase space and $B_{tz}$ field component at the same time for different upstream ion $\beta_i$ values used in Figures 1 and 6 ($\beta_i$ = 0.022, 0.177 and 0.35). It clearly appears that for low $\beta_i$ (case a), reflected ions have a very coherent motion (narrow ring) as described by the well defined trapping loop (vortex) in the $p_{xi} - x$ plot at the beginning of the reflection. This coherence forces these ions to accumulate over a narrow spatial range at a foot length distance from the ramp; it results that ramp and foot are well separated. This accumulation is suitable for building up a peaked-like foot which itself reflects at later times new incoming ions before these reach

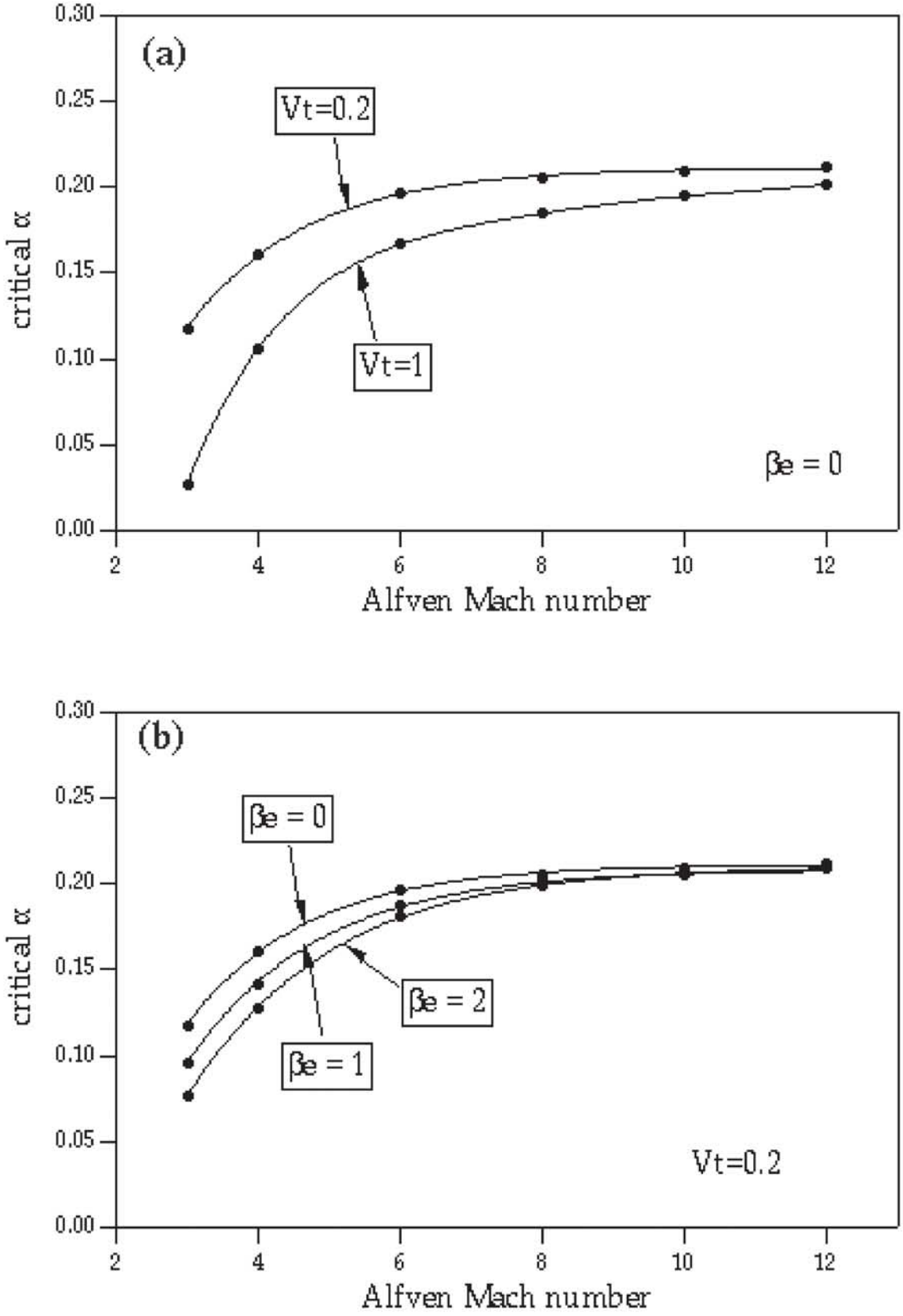


**Figure 5.** Similar to Figure 4, except with different values of the upstream ion temperature (case a) and of the electron $\beta_e$ (case b).

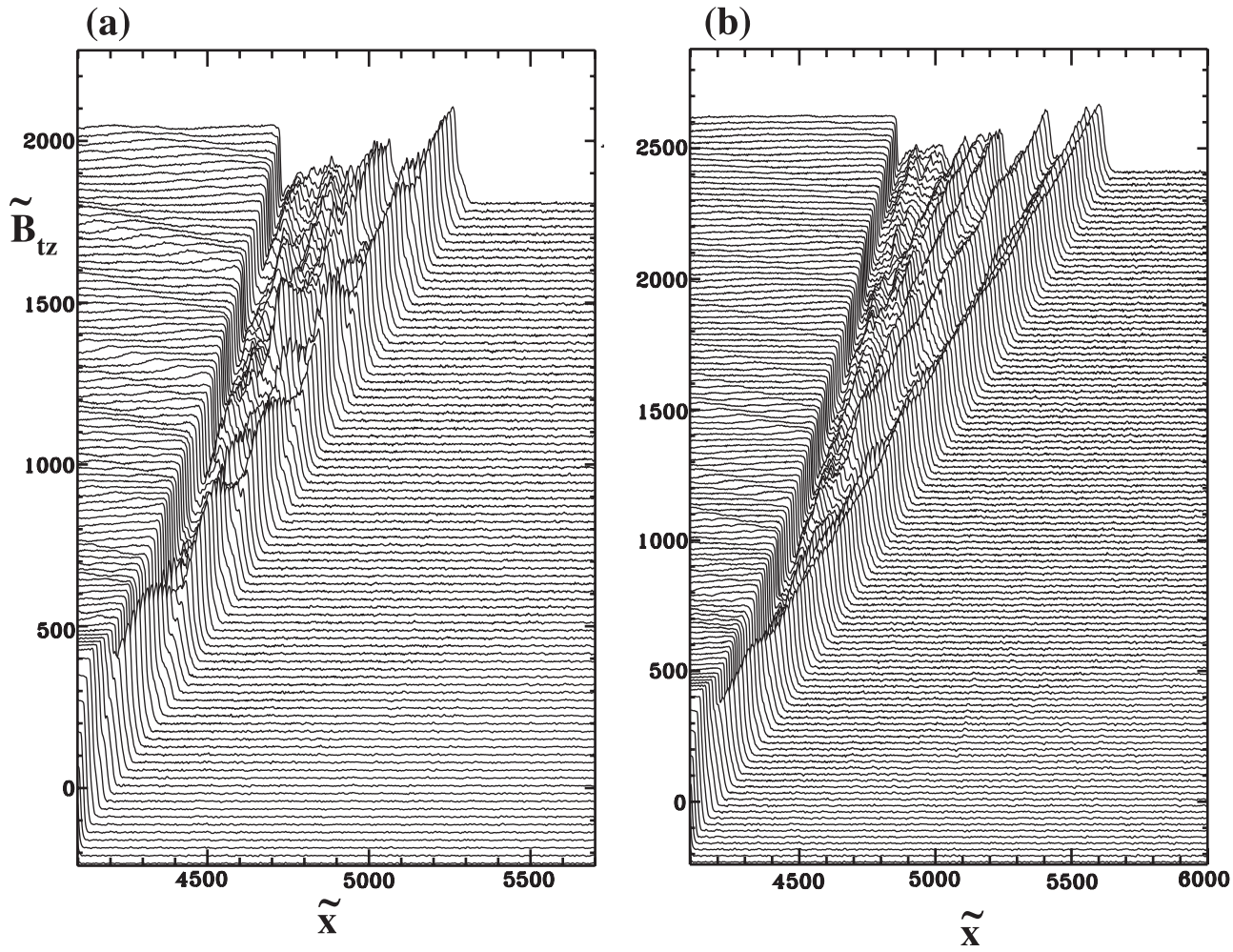


**Figure 6.** Similar to Figure 1, except $\beta_i$ = 0.177 and 0.35 respectively for cases a and b.

the ramp (as seen in $B_{tz}$ field profile). In contrast, as $\beta_i$ increases (case b), this coherence is progressively lost to be replaced by a stochastic motion; reflected ions are more diffuse. For high $\beta_i$ (case c), reflected ions are immediately diffuse when passing through the resonant region (when these reach the shock velocity) and accumulate over a much wider spatial range spreading within the ramp region; as a consequence, foot and ramp are mixed together and cannot be clearly distinguished (to see $B_{tz}$ profile). No peaked-like foot is formed to decelerate new incoming ions. Then, the self reformation is not only depending on the percentage of reflected ions but also on the width of the spatial range over which these ions accumulate.

[34] In terms of modeling, coherent motion means that reflected ions (for low $\beta_i$) can be described by one narrow ring population (with a relatively weak thermal velocity). In contrast, the diffuse reflected ions should be modeled differently, since the use of a narrow ion ring in perpendicular velocity space is not valid any more for high $\beta_i$ case. For this case, one has also to take into account the relative proximity of the thermal velocity of the incident ions (in particular the tail part of the distribution) and the bulk motion of reflected ions. Then, the increase of the upstream $\beta_i$ does not lead only to a simple increase of the downstream $\beta_i$, but makes also the modeling used herein questionable. As a consequence, our present model is only adapted for the low $\beta_i$ case; more precisely, this validity holds as long as a single narrow ring population can be used for describing the first part of the ion gyromotion during the reflection, i.e. for ions with velocities between the shock velocity and the maximum velocity value reached at the trapping loop (as in Figure 2). This condition is important for initiating a peak-like foot away from the ramp, and is related to the ratio of the shock velocity versus upstream ion thermal velocity. This ratio strongly controls the possible formation of the trapping loop. In other words, when this ratio is large (relatively low $\beta_i$ and/or $M_A$ high enough so that $v_{shock} \gg V_{ti}$), the motion of reflected is coherent and the present model can apply; however, when this ratio is weak (relatively low $M_A$ - but still above $M_A^*$- and/or high $V_{ti}$ so that $v_{shock}$ is only a few times $V_{ti}$), the motion of reflected ions is quite diffuse and the present model cannot apply. Introducing an improved model to describe the reflected ions for high $\beta_i$ case requires a more sophisticated theoretical treatment which is out of scope of the present paper.

## 5. Conclusions

[35] In this paper we analyzed the shock front nonstationarity of super-critical perpendicular shocks by examining

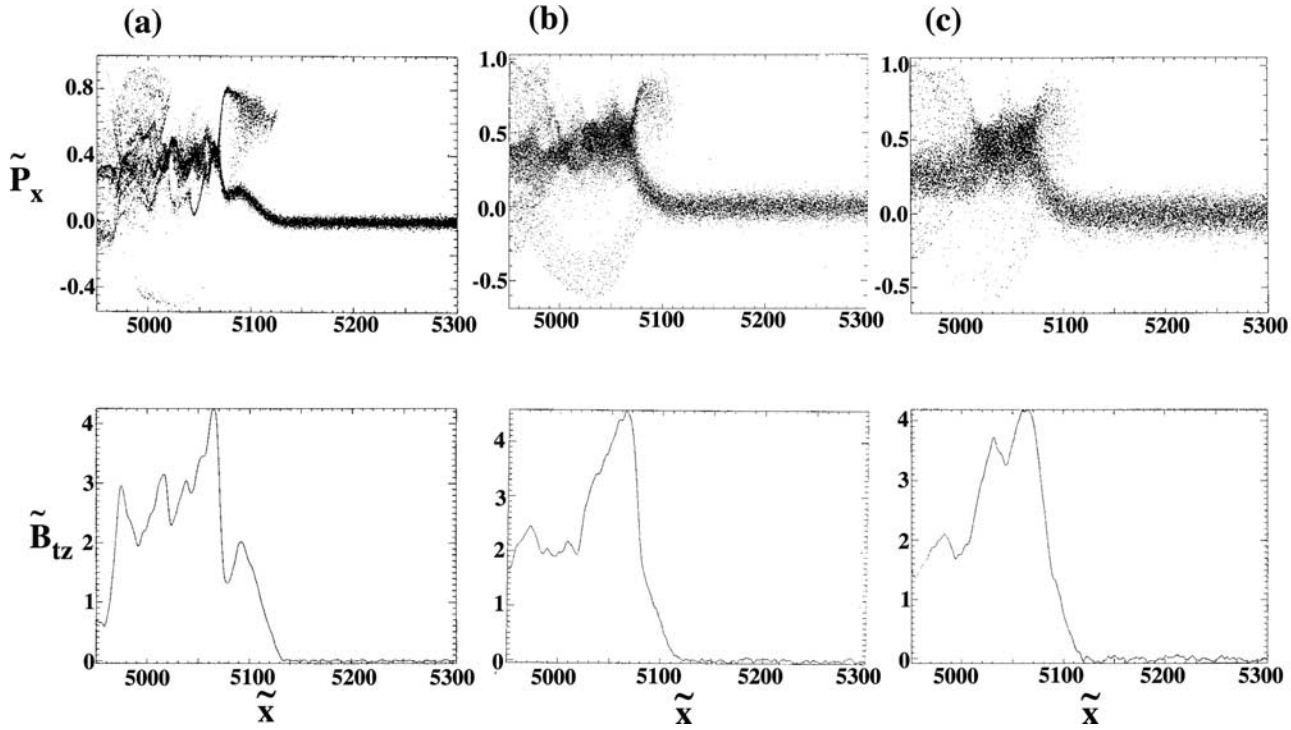


**Figure 7.** Ion phase space $\tilde{p}_{xi} - \tilde{x}$ and corresponding x-profile of the main magnetic field component for three different runs. All plots are defined around the shock front within the same spatial range ($4950 < \tilde{x} < 5300$), at the same time $\tilde{t} = 1728$. All plasma parameters are identical (Table 1) except $\beta_i = 0.022$, 0.177 and 0.35 respectively defined for cases a, b, and c.

the coupling between "incoming" and "reflected" ion populations. For a given set of parameters, we sought for a self-consistent, time-stationary solution of the coupling between ion streams and the electromagnetic field. If such a solution is found, the shock is stationary; otherwise, the shock is nonstationary, and we argued that it corresponds to a self-reforming shock front often observed in full particle simulations of quasi-perpendicular shocks. We defined a critical $\alpha_{crit}$ below (above) which the shock is stationary (nonstationary). The shock can be nonstationary even for relatively low $M_A$ (2–5). For a moderate $M_A$ (5–10), the critical value $\alpha_{crit}$ is about 15 to 20%, and for very high $M_A$ (>10), $\alpha_{crit}$ saturates around 20%.

[36] The structure of the perpendicular supercritical shocks was discussed by *Leroy* [1983], which shows the morphology of reflected gyrating ion streams and the dependence of the shock structure with Mach number. Our present model differs from his model in that the coupling between the incoming ions, the reflected ions, and the field is self-consistently treated (in Leroy's model, trajectories of the ion streams are computed but their interaction with the field is not considered), and that in our model the fraction of reflected to the incoming ion densities is given as an external parameter (in contrast to the Leroy's model, in which $\alpha$ is self-consistently determined from flux conservation relations across the shock).

[37] By making runs with varying $\alpha$, we showed explicitly that the shock stationarity is strongly dependent on the value of $\alpha$. On the other hand, one has to stress that, for a real (self-consistent) shock, $\alpha$ is self-consistently determined as a function of upstream parameters. Then, the diagram of Figure 4 does not mean that several values $\alpha$ can be determined for a given value of $M_A$. One should also keep in mind that the self-reformation has been also evidenced in previous 2-D full particle simulations in comparable supercritical Mach regimes (*Lembège and Savoini* [1992], for a 2-D planar shock; *Savoini and Lembège* [1999, 2001] for a 2-D curved shock). This means that other dissipation mechanisms carried self-consistently by cross-field currents instabilities (2-D effects) are not strong enough to suppress the shock front nonstationarity, and that ion reflection remains a key dissipation process.

[38] Results deduced from the present model may be of great importance for accounting for or predicting conditions in which the front of the terrestrial bow shock may suffer self-reformation. This feature can be analyzed with the help of several satellites located at distances each other large enough to identify different signatures of fields components during the shock front crossing, as done by Cluster-2 mission. Such local signatures have been well reproduced in a recent computer generated movie where four "virtual" satellites have been inserted into results of 2-D full particle simulations, in order to mimic the shock front crossing performed by Cluster-2 multisatellites mission performed by B. Lembège, P. Martel, and P. Savoini in 2001 under the title *Evidence of shock front turbulence by "virtual" satellites: CLUSTER-II mission*. These diagnosis are now under active investigation in order to analyze Cluster-2 experimental data. In addition, previous hybrid simulations did not evidence such self-reformation over a foot length scale but rather some unstationarity of the front located at the overshoot (local fields fluctuations only). At least, this point can be explained by the fact that higher values of ion beta have been used; present full particle simulation results also

show that self-reformation disappears and is replaced by fields fluctuations at the overshoot as $\beta_i$ increases, or even the shock front becomes totally stationary for higher $\beta_i$. Then, such a reformation should be more systematically evidenced with appropriate conditions, since it has been already observed in unpublished hybrid simulations results (Simonet, private communication, 1990). As suggested by *Lembège and Simonet* [2001], some readjustment of the plasma parameters and of grid size could account for the transition between absence and presence of self-reformation in hybrid simulation results. On the other hand, let us remind that most of previous hybrid simulations are based on rough grid resolution (the grid size is of the order of the ion inertia length). The impact of the grid resolution on the self-reformation has been only recently analyzed by *Hellinger et al.* [2002], who have shown that the self reformation clearly appears (disappears) when the used spatial grid resolution is high enough (too low).

[39] Moreover, a comparison with results issued from full particle simulations confirms that the present model applies mainly to the low $\beta_i$ case, as long as the motion of reflected ions is coherent enough to be described appropriately by a single ion ring population (at least on the first part of their gyromotion). Simulation results indicate that this condition holds when the shock velocity is much higher than the thermal velocity of incident ions. An extensive development of the model will be necessary in the near future, in order to describe the full diffuse motion of reflected ions evidenced for the high $\beta_i$ case.

[40] **Acknowledgments.** Full particle simulation runs have been performed on the NEC *SX*5 of the supercomputer center IDRIS located at Orsay. Thanks are addressed to J. M. Teuler and Nicolas Grima for their helpful computing assistance. This work has been performed under the auspices of the International Space Sciences Institute (ISSI, Bern) which is thanked for his financial support and hospitality.

[41] Shadia Rifai Habbal thanks K. Papadopoulos and another referee for their assistance in evaluating this paper.

## References

Biskamp, D., and H. Welter, Ion heating in high-mach number, oblique, collisionless shock waves, *Phys. Rev. Lett.*, *28*, 410–413, 1972.

Hellinger, P., P. Travnicek, and H. Matsumoto, Reformation of perpendicular shocks: Hybrid simulations, *Geophys. Res. Lett.*, *29*(24), 2234, doi:10.1029/2002GL015915, 2002.

Lembège, B., and J. M. Dawson, Self-consistent study of a perpendicular collisonless and nonresistive shock, *Phys. Fluids*, *30*, 1767–1788, 1987.

Lembège, B., and P. Savoini, Nonstationarity of a two-dimensional quasi-perpendicular supercritical collisionless shock by self-reformation, *Phys. Fluids*, *4*, 3533–3548, 1992.

Lembège, B., and F. Simonet, Hybrid and particle simulations of an interface expansion and of collisonless shock: A comparatible and quantitative study, *Phys. Plasmas*, *8*(9), 3967–3981, 2001.

Leroy, M. M., Structure of perpendicular shocks in collisionless plasmas, *Phys. Fluids*, *26*, 2742–2753, 1983.

Leroy, M. M., C. C. Goodrich, D. Winske, C. S. Wu, and K. Papadopoulos, Simulation of a perpendicular bow shock, *J. Geophys. Res.*, *86*, 1269–1272, 1981.

Leroy, M. M., D. Winske, C. C. Goodrich, C. S. Wu, and K. Papadopoulos, The structure of perpendicular bow shocks, *J. Geophys. Res.*, *87*, 5081–5094, 1982.

Savoini, P., and B. Lembège, Full curvature effects of a collisionless shock, *Adv. Space Res.*, *14*(1), 13–22, 1999.

Savoini, P., and B. Lembège, Two-dimensional simulations of a curved shock: Self-consistent formation of the electron foreshock, *J. Geophys. Res.*, *106*, 12,975–12,992, 2001.

T. Hada and M. Oonishi, Kyushu University, 6-1 Kasuga-Koen, Kasuga, Fukuoka 816-8580, Japan. (hada@esst.kyushu-u.ac.jp)

B. Lembège and P. Savoini, CETP/UVSQ, 10-12, Av. de l'Europe, 78140 Vélizy, France. (Bertrand.LEMBÈGE@cetp.ipsl.fr; Philippe.SAVOINI@cetp.ipsl.fr)